Simulation of anisoplanatism of an adaptive optical system in the turbulent atmosphere

A.V. Koryabin, M. Moradi, and V.I. Shmalgausen

Moscow State University

Received January 28, 2005

A designed software for simulating the effect of anisoplanatism on operation of a phase-conjugation adaptive optical system in turbulent atmosphere is described. Atmospheric turbulence is simulated with a system of moving random phase screens with a preset statistics. The software developed allows calculation of instantaneous and averaged errors of phase correction at different angular separations of the reference source (beacon) and the observation site in a wide range of parameters of the adaptive system and atmospheric inhomogeneities. Such an approach enables one both to estimate residual errors of aberration compensation in the adaptive system and to calculate instantaneous characteristics of the entire system, namely, the point spread function (PSF) and the optical transfer function (OTF), as well as to estimate the angular dimension of the isoplanatism region.

Introduction

A quality of image of some object observed through a perturbed atmosphere, can be enhanced in the receiving optical device by methods of adaptive optics. An adaptive system enables a compensation of phase aberrations occurring due to fluctuations of refractive index of the turbulent medium, but such compensation is effective only within the limits of the isoplanatism zone. Anisoplanatism of an adaptive optical system[1] is one of the factors restricting the correctability of medium-distorted images of extended objects.

This effect is caused by the fact that atmospheric inhomogeneities are three-dimensional while adaptive optical systems corrects the phase in one plane determined by a wavefront (WF) corrector position. If an object is larger than the isoplanatism zone (extended object) then optical paths of waves from different object's points differ significantly. Hence, phase aberrations of these waves also differ. This presents additional difficulties both to registration of aberrations and to their compensation with a phase corrector.

As the angle between directions of an object's observation point and a reference source (beacon) increases, correlation between phase aberrations, cumulative along these directions, decreases, that results in incomplete correction of images of regions far distant from the beacon. This effect strongly depends on statistics of atmospheric inhomogeneities and their altitude distribution. All this complicates the analysis of an adaptive optical system operation in the atmosphere.

Usually, the analysis of the adaptive correction efficiency under anisoplanatism conditions is confined to the Kolmogorov turbulence model and the approximation of homogeneous atmosphere or homogeneous layer.[2] Although such an approximation is widely used for atmospheric turbulence description, sometimes it poorly agrees with experimental data, and in this case it is necessary to apply more complicated methods.[3] The simulation technique allows overcoming these difficulties.

1. Simulation technique

Computer simulation technique allows one to analyze an adaptive optical system operation with different turbulence models and compare the obtained results. Advantages of computer techniques manifest themselves best, when accounting for atmosphere inhomogeneity along the beam propagation path and when the turbulence is drifted by the crosswind. All this conditions, typical for *in situ* operation, are difficult to be taken into account in analytical approaches, but are easily realizable in computer models.

The numerical simulation technique[4] allows one to overcome the majority of difficulties and to obtain typical realizations of phase aberrations in some adaptive system under anisoplanatism conditions. Another advantage is a possibility of on-line assessment of the system's isoplanatism region depending on the system parameters and the atmospheric model. A simple estimate of the isoplanatism angle[1]

$$\theta_0 \cong 0.6\frac{r_0}{H}$$

(where r_0 is the Freed radius and H is the effective thickness of the turbulent layer) does not account for receiving system's finite aperture influence and gives very underestimated results. Usually, the aperture effects are calculated numerically.[3,5] Within the modeling technique, the isoplanatism angle can be estimated by the Strehl criterion variation at an ideal phase conjugation. In the case, when angular separation increases from 0 to θ_0, the corresponding decrease of the Strehl factor is $1/e \approx 0.37$.

In this work, we describe a program for simulating the effect of anisoplanatism on operation of a phase-conjugation adaptive optical system under conditions of atmospheric turbulence drifted by crosswind, and present typical results.

Simulating the anisoplanatism effect is directed to obtaining the intensity distribution at the adaptive system outlet, i.e., the image corrected by some algorithm. The model in use should allow one to calculate instant (not averaged) phase distributions for a reference wave in the receiving aperture plane, the WF sensor response and its output signals, as well as the introduced phase correction.

These data make it possible to calculate the residual correction error and estimate a quality of image of any object's region. The construction of the point-spread function (PSF) is a key point in conversion from a random phase distribution in the aperture plane to the image.

In a number of works on adaptive optics,[6,7] the PSF, which shape corresponds to a point source image, serves as the fundamental characteristic for estimation of compensation efficiency and image quality. In incoherent optics, this function is the main image-quality criterion. Its Fourier transform – the optical transfer function (OTF) – is often used alternatively.

Instant PSF and instant OTF are random functions corresponding to the "frozen" atmosphere snapshot. Average characteristics of an imaging system are calculated theoretically as follows: the long-exposure PSF can be obtained via averaging the instant one, while the short-exposure one[3,8,9] – via centering snapshot images followed by averaging. In actual experiments, the averaging is usually performed over a finite time span. Such functions can be easily obtained in a model experiment and they well illustrate a possible image quality.

A distinctive feature of an anisoplanatic system is the parametric dependence of PSF and OTF shapes on coordinates of the observed area.

2. Structure and composition of the program

The program consists of the following blocks: a) simulation of light wave propagation in turbulent atmosphere; b) simulation of Hartmann sensor operation, which reshapes the phase profile of a reference source wave; c) phase correction of a reference source wave, and d) calculation and processing of residual errors. The program structure is presented in Fig. 1.

To simulate atmosphere, the phase screen method was used. The turbulent atmospheric layer between the object and the receiving aperture was represented as several thin phase screens. Waves from the reference source (*1*) and some point of the observed object (*2*) (separated by the angle θ) were registered separately within the receiving aperture of the diameter D. The plane passing through directions to the reference source and the observation point made the angle α with the direction of a prevailing wind (x axis). The wave propagation from a screen to screen was considered free of distortions and getting only casual phase incursions on screens. The light intensity was supposed invariable (phase approximation).

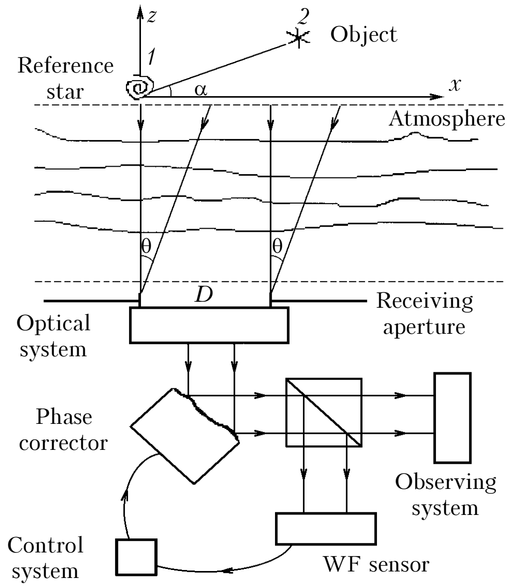

Fig. 1. Calculation scheme of the atmospheric model.

The turbulent atmosphere with different properties can be modeled via varying the distribution of phase incursions on screens. The screens were realized by the well-known technique[10] providing for screen generation depending on different parameters and turbulence spectra. Usually, four screens were used capable of moving across the observation direction with a certain speed (wind simulation).

As a WF analyzer, the Shack–Hartmann sensor was simulated.[11] Lens raster was situated in the receiving aperture plane with an apodizing diaphragm in front of each lens. The focal plane intensity distribution was calculated from phase distortions of a registered wave within each lens (subaperture) while center-of-gravity shifts of focal spots served as a measure of WF local slopes within each subaperture. Zernike coefficients for reference φ_0 and subject φ_t waves were least square recovered from the measured local slopes:

$$\varphi_0 = \sum_{i=1}^{N} a_i^0 Z_i(\mathbf{r}), \quad \varphi_t = \sum_{i=1}^{N} a_i^t Z_i(\mathbf{r}), \qquad (1)$$

where $Z_i(\mathbf{r})$ is the Zernike polynomial and N is the total number of accounted modes.

Two correction techniques were realized in the adaptive system: the phase conjugation and the weighted conjugated correction.[13] In the first case, the correcting phase makeweight φ_c was equal in magnitude and opposite in sign to the measured random phase of the reference source:

$$\varphi_c = -\sum_{i=1}^{n} a_i^0 Z_i(\mathbf{r}). \quad (2)$$

When correcting, only a limited number $n \le N$ of terms of expansion in Zernike polynomials was considered; thus, the number of degrees of freedom of the corrector in use was taken into account.

Within the second technique, phase makeweights minimized the residual squared error:

$$\varphi_c = -\sum_{i=1}^{n} a_i^0 K_i(\theta) Z_i(\mathbf{r}), \quad (3)$$

where $K_i(\theta)$ is the correlation coefficient of the ith mode of phase shapes for waves propagating at the angle θ to each other.

The phase shape of a corrected wave from the object was analyzed and residual aberrations were determined depending on magnitude of the angular separation θ and the order of correction n. The residual aberration coefficients were used for PSF and OTF calculation. The case of total ("ideal") phase-conjugated correction was considered as well, when distortions were compensated in all measured modes: $n = N$. In this case the residual error depends only on the system anisoplanatism and allows estimation of the isoplanatism region width.

The model allows detection of time variations of aberration coefficients in the same way as in an adaptive system when observing through the moving turbulent layer. Therewith, it is possible to record optical system parameters, both instant (corresponding to frozen inhomogeneities) and averaged over the preset time interval. The maximal averaging interval is restricted by permissible dimensions of the moving phase screens and the required calculation time.

3. Results

Figure 2 shows fluctuations of the residual squared correction error in view of 20 Zernike modes minus slopes:

$$\sigma^2 = \sum_{i=3}^{20} (a_i^0 - a_i^t)^2. \quad (4)$$

Time fluctuations occurred when modeling the turbulent layer drift by the crosswind of the speed v. The squared residual error is time-averaged.

As is seen, characteristic behavior of the phase error agrees with the Greenwood frequency period v/r_0. Noticeably long time periods can be distinguished, in which aberrations are substantially smaller than the mean value. This demonstrates a possibility of obtaining high-quality short-exposures through the turbulent atmosphere provided that the moment of photographing is chosen auspiciously.[14]

The normalized squared compensation errors ε_{0i}^2 versus the angle θ, averaged over 50 measurements, for few different aberrations are presented in Fig. 3:

$$\varepsilon_{0i}^2 = \frac{\left(a_i^0 - a_i^t\right)^2}{(a_i^0)^2}. \quad (5)$$

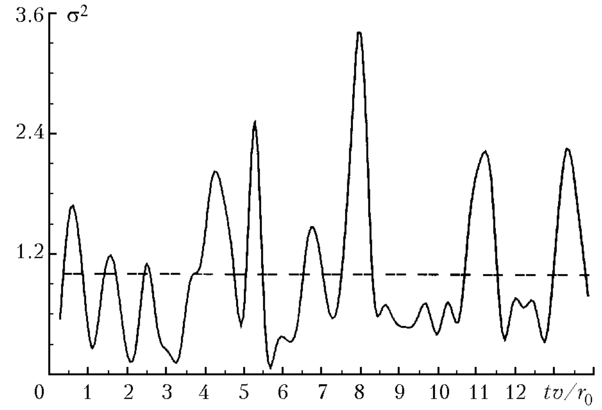

Fig. 2. Time fluctuations of the residual squared correction error at crosswind drift of turbulence. The dashed line corresponds to the average squared error (four screens, $\alpha = 0$ rad, $D/r_0 = 18$).

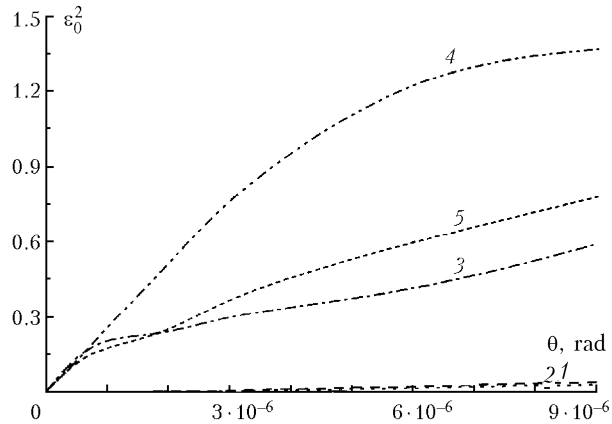

Fig. 3. Normalized correction error for different aberrations depending on separation of the observation point and the reference source: X-slope (*1*), Y-slope (*2*), defocusing (*3*), X-coma (*4*), and Y-coma (*5*) (four screens, $\alpha = 0$ rad, $D/r_0 = 18$).

The correction was performed by the phase conjugation method. All curves were normalized to the square of the corresponding mode without compensation. Calculations were carried out for a homogeneous turbulent layer with the Kolmogorov spectrum. The region of good slope compensation (curves *1* and *2*) is evidently wider than that of high order aberrations. This feature is in a good agreement with theoretical models. It is also seen, that the residual error in the adaptive system can exceed the error in the system free of correction ($\varepsilon_0^2 > 1$).

A similar result was obtained in Ref. 15 when analyzing the error in a long-delay adaptive system: if the delay in a controlling circuit exceeds the correlation time of phase inhomogeneities at the receiving aperture, then the error can be twice as large as in the system free of correction. This can happen in our case as well due to total loss of correlation ($K_i(\theta) \approx 0$) at a large angular separation θ. Irregular behavior of the curves is connected with insufficient number of averagings.

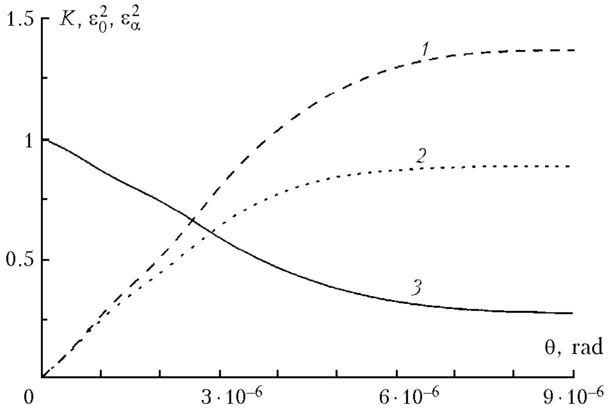

Fig. 4. Residual squared astigmatic error at phase conjugation (*1*) and at effective weight correction (*2*). The curves are normalized to the error in a non-corrected system. Curve *3* corresponds to the correlation coefficient. $D/r_0 = 18$.

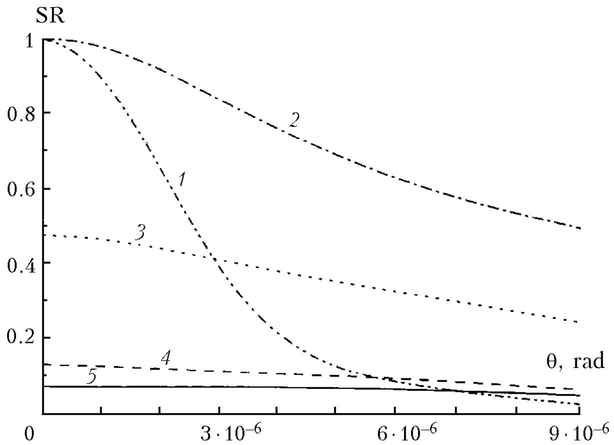

Fig. 5. Dependence of the Strehl number SR on angular separation of sources at different number of corrected Zernike modes: $D/r_0 = 12$ (*1*) and $D/r_0 = 5$ (*2–5*); *1* and *2* correspond to total correction of all modes, correction of nine lower Zernike modes (*3*), correction of five lower Zernike modes (*4*), and without correction (*5*). $\theta_0 = 1.5 \cdot 10^{-5}$ rad (*2–5*) and $3 \cdot 10^{-6}$ (*1*).

Figure 4 demonstrates the effect of the weighted correction, when each correcting mode of the reference source is considered with its effective weight according to Eq. (3). As was shown in Ref. 13, at such a correction, the residual error never exceeds the error in a non-corrected system even in the case of one reference source. Because of usual lacking of *a priori* data on correlation coefficients $K_i(\theta)$ for Zernike modes necessary for the algorithm, its realization is difficult. In the model, the unknown correlation coefficients $K_i(\theta)$ are determined through analysis of phase fluctuations during the adaptive system operation. In Fig. 4, curve *1* corresponds to the residual error of one of the aberrations (astigmatism) at phase conjugation, curve *2* — at effective weight correction. Solid curve *3* shows the angular dependence of the correlation coefficient estimated by 50 different positions of phase screens. As is seen, the weight correction is much more efficient than the phase conjugation under great angular separation.

Figure 5 shows the Strehl number SR dependence on the angular separation of sources at different number of corrected Zernike modes. Upper curves correspond to total correction at $D/r_0 = 5$ and 12 giving θ_0-angle estimates $1.5 \cdot 10^{-5}$ and $3 \cdot 10^{-6}$ rad, respectively.

Three-dimensional OTF patterns for an adaptive phase-conjugation system are presented in Fig. 6 for the cases of the object location inside ($\theta = 0.05 \cdot 10^{-6}$) and outside ($\theta = 0.9 \cdot 10^{-6}$) the region of isoplanatism.

As is seen from Fig. 6, even in the case of ideal phase correction, the OTF is significantly deformed outside the isoplanatism region, contracting along the direction x of separation between a reference source and an observed object, while inside this region it is close to a diffraction-limited system.

The PSFs without correction and at total correction are presented in Fig. 7 at different observation angles. The PSF of the corrected system is evidently close to a diffraction-limited one inside the isoplanatism region; and at angles exceeding the isoplanatism angle, it disintegrates into individual narrow peaks covering a considerable area.

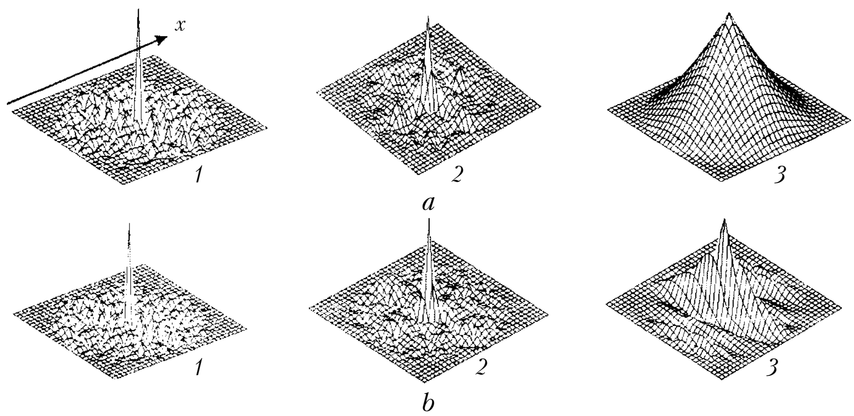

Fig. 6. OTF of an adaptive phase-conjugation system ($D/r_0 = 12$) for $\theta = 0.05 \cdot 10^{-6}$ (*a*) and $0.9 \cdot 10^{-6}$ (*b*): without correction (*1*); correction of nine lower Zernike modes (*2*); total correction of all registered modes (*3*). Isoplanatism angle in this case is $3 \cdot 10^{-6}$ rad.

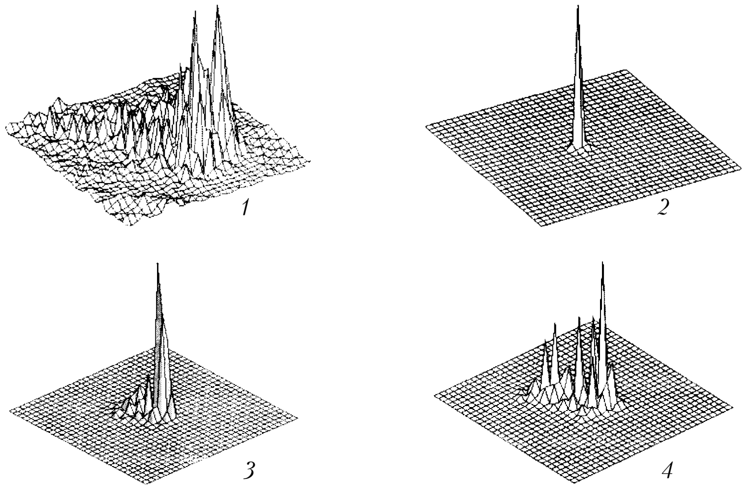

Fig. 7. PSF of an adaptive phase-conjugation system (D/r_0 = 12): without correction (*1*); for $\theta = 0.05 \cdot 10^{-6}$ (*2*); for $\theta = 0.3 \cdot 10^{-6}$ (*3*); and for $\theta = 0.9 \cdot 10^{-6}$ (*4*). Isoplanatism angle is $3 \cdot 10^{-6}$ rad.

Conclusion

The designed software allows calculation of instant and averaged phase correction errors at different angular separations of the reference source and the observation site within a wide range of adaptive system parameters and atmospheric inhomogeneities. This makes possible to calculate the instant and average system parameters, i.e., the point-spread function and the optical transfer function, as well as estimate the angular dimension of the isoplanatism region.

References

1. D.L. Fried, J. Opt. Soc. Am. **72**, 52–61 (1982).
2. V.I. Shmalgausen and N.A. Yaitskova, Atmos. Oceanic Opt. **9**, No. 11, 930–935 (1996).
3. H. Zhang, F. Yin, B. Xu, and W. Jiang, Opt. Engineering **42**, No. 8, 2190–2196 (2003).
4. V.P. Lukin and B.V. Fortes, *Adaptive Beam and Image Formation in the Atmosphere* (Publishing House of SB RAS, Novosibirsk, 1999), 214 pp.
5. P.H. Hu, J. Stone, and T. Stanly, J. Opt. Soc. Am. **11**, 347–357 (1994).
6. R.W. Wilson and C.R. Jenkins, Mon. Notic. Roy. Astron. Soc. **268**, 39–61 (1996).
7. G. Molodij and J. Rayrole, Astron. & Astrophys. Suppl. **128**, 229–244 (1998).
8. R.E. Hufgenagel and N.R. Stanly, J. Opt. Soc. Am. **54**, 52–61 (1964).
9. D.L. Fried, J. Opt. Soc. Am. **56**, 1372–1379 (1966).
10. S.S. Chesnokov, V.P. Kandidov, S.A. Shlenov, and M.P. Tamarov, Proc. SPIE **3432/25**, 14 (1998).
11. Ben C. Platt and Roland Shack, J. of Refract. Surgery **17**, Sep./Oct., 573–577 (2001).
12. M.A. Vorontsov, A.V. Koryabin, and V.I. Shmalgausen, *Controllable Optical Systems* (Nauka, Moscow, 1988), 272 pp.
13. V.I. Shmalhausen and N.A. Iaitskova, Proc. SPIE **4338**, 97–106 (2000).
14. S. John and M.A. Vorontsov, *Proc. of Intern. Conf. on Multimedia and Expo. 2003. ICME'03* (2003), Vol. 1, pp. 6–9.
15. V.P. Lukin, *Adaptive Atmospheric Optics* (Publishing House of SB RAS, Novosibirsk, 1986), 286 pp.